

Synthesis, ^{89}Y and ^{51}V -NMR of Er-doped zircon-type YVO_4 and LuVO_4

R. Amantea, P. Ghigna, P. Mustarelli*, V. Tartara

Dipartimento di Chimica Fisica "M. Rolla", and IENI-CNR, Via Taramelli 16, IT-27100 Pavia, Italy

Received 16 December 2004; received in revised form 7 March 2005; accepted 11 March 2005

Abstract

$\text{Y}_{0.99}\text{Er}_{0.01}\text{VO}_4$ and $\text{Lu}_{0.99}\text{Er}_{0.01}\text{VO}_4$ zircon-type compounds have been synthesized by solid-state reaction starting from the parent oxides. The obtained materials are single phase, well crystallized and homogeneous in the chemical composition.

The magic angle spinning-NMR characterization points toward the substitutional nature of erbium on the rare earth site. The isotropic chemical shift of ^{89}Y in an orthovanadate is reported for the first time.

© 2005 Elsevier Inc. All rights reserved.

Keywords: Zircon-type materials; Solid-state reactions; Luminescent materials; ^{51}V and ^{89}Y MAS-NMR

1. Introduction

Rare earth orthovanadates are of interest due to their unusual magnetic properties and as useful hosts for luminescent cations such as Nd^{3+} , Er^{3+} , etc. In addition, these compounds have been used as model systems for the investigation of phase transitions for the ABO_4 -type structure: in fact, the zircon-type vanadates are reported to undergo to a reconstructive transformation to the denser scheelite-type structure at pressures around few kilobars and $T < 600^\circ\text{C}$. The crystal structure at room temperature of these compounds has been widely investigated in the past, both with single crystal X-ray and with neutron powder diffraction [1–6]: the space group is $I4_1/amd$ (no. 141, origin in $8c$ 0.2 m) with the V(V) ions in the $4b$ position (0 1/4 3/8), the RE(III) ions in the $4b$ position (0 3/4 1/8) and the oxide ions in the $16h$ position (0yz) with $y \cong 0.4$ and $z \cong 0.2$, depending of the nature of the rare earth. The structure can be pictorially described as built up by chains of alternating edge sharing VO_4 tetrahedra and REO_8 bisdisphenoids. These chains run parallel to the c -axis,

while the bisdisphenoids themselves form “zigzag” chains running parallel to the a -axis. The VO_4 tetrahedra are slightly elongated as the edges shared with the bisdisphenoids are shorter than those not shared. In any case, the V–O bond length is unique and $\cong 1.71 \text{ \AA}$, while the eight RE–O bonds subdivide in two sets: four RE–O short bonds shared with other bisdisphenoids (bond length $\cong 2.1$ – 2.4 \AA , depending on RE) and four RE–O long bonds shared with the tetrahedra (bond length $\cong 2.4$ – 2.5 \AA , depending on RE) [6]. In the present study, we have synthesized high-quality powders of YVO_4 and LuVO_4 both doped with Er^{3+} (1% atomic ratio) by solid-state reaction. The erbium doping was employed in view of possible applications of these compounds as luminescent materials. The local structure of the compounds was investigated by ^{51}V and ^{89}Y magic angle spinning (MAS)-NMR.

2. Experimental

$\text{RE}_{1-x}\text{Er}_x\text{VO}_4$ (RE = Y, Lu) samples with $x = 0.01$ were synthesized by solid-state reaction starting from stoichiometric amounts of RE_2O_3 , V_2O_5 and Er_2O_3 of

*Corresponding author. Fax: +39 0382 987575.

E-mail address: mustarelli@matsci.unipv.it (P. Mustarelli).

high purity (Aldrich >99.99%). The rare earth oxides are known to react promptly with moisture and carbon dioxide of the atmosphere. Therefore, immediately before to weight the proper amount of each rare earth oxide, a thermogravimetric analysis was carried out on it (by means of a TA 2000 apparatus), and a correction for the weight loss (around 1%) has been applied. The powders were thoroughly mixed in acetone and then pressed to pellets and allowed to react at 800 °C for a total time of 12 h in air. X-ray powder diffraction (XRPD) and electron micro-probe analysis (EMPA) inspections were performed to check the chemical and phase purity of the obtained materials. XRPD patterns were acquired on a Bruker D8 diffractometer equipped with a Cu anticathode, adjustable divergence slit, graphite monochromator on the diffracted beam and proportional detector. The lattice constants were determined by minimizing the weighted squared difference between calculated and experimental Q_i values, where $Q_i = 4 \sin^2 \theta_i / \lambda_i^2$ and $\text{weight} = \sin(2\theta_i)^{-2}$. Instrumental aberrations were considered by inserting additional

terms into the linear least-square-fitting model [7]. EMPA measurements were carried out using an ARL SEMQ scanning electron microscope, performing at least 10 measurements in different regions of each sample. According to EMPA and XRPD, the above synthetic procedure gave single-phase materials with homogeneous composition. The SEM images of the two compounds are shown in Fig. 1, to display their grain shape and size distribution.

^{51}V MAS-NMR spectra were collected with an AMX400WB spectrometer (Bruker, Germany, $B_0 = 9.4\text{ T}$), at the Larmor frequency of 105.19 MHz. The spectra were acquired with a 4 mm probehead (Bruker), equipped with cylindrical zirconia rotors and a boron nitride stator. The samples were spun at 12 kHz and the data were averaged over 12 k acquisitions using a single-pulse sequence, with a 15° pulse of 0.5 μs , a recycle time of 1 s, and a spectral width of 1 MHz. The baseline distortions were corrected by a linear prediction of the first 10 points, followed by baseline correction (WINNMR package, Bruker). The best-fit procedures were performed with the WSOLIDS package [8].

^{89}Y spectrum was acquired at 19.6 MHz, using a 7 mm probehead (Bruker) equipped with cylindrical zirconia rotors and a boron nitride stator. The sample was spun at 7 kHz and the data were averaged over ~ 1500 acquisitions using a Hahn-echo sequence, with a 90° pulse of 10 μs , a 180° pulse of 20 μs and a recycle time of 35 s. The spectrum was referenced to YCl_3 .

3. Results and discussion

3.1. X-ray powder diffraction

Figs. 2 and 3 show the XRPD pattern of $\text{Y}_{0.99}\text{Er}_{0.01}\text{VO}_4$ and $\text{Lu}_{0.99}\text{Er}_{0.01}\text{VO}_4$, respectively. As it is seen all the diffraction effects can be indexed according to the zircon-type vanadate structure. In addition, both compounds appear to be very well crystallized, the splitting between the α_1 and α_2 being clearly visible above $2\theta = 25^\circ$. This is confirmed by the SEM images shown in Fig. 1. The lattice constants obtained by the procedure described in the experimental are $a = 7.119(2)$, $c = 6.290(2)$ for the $\text{Y}_{0.99}\text{Er}_{0.01}\text{VO}_4$ compound and $a = 7.027(2)$, $c = 6.233(2)$ for the $\text{Lu}_{0.99}\text{Er}_{0.01}\text{VO}_4$ compound, in excellent agreement with previous powder neutron diffraction measurements on the un-doped compounds [6].

3.2. NMR

^{51}V ($I = 7/2$) solid-state NMR spectroscopy is now considered a technique-of-choice for the characterization of local structure in vanadates, which are of interest for relevant technological applications including

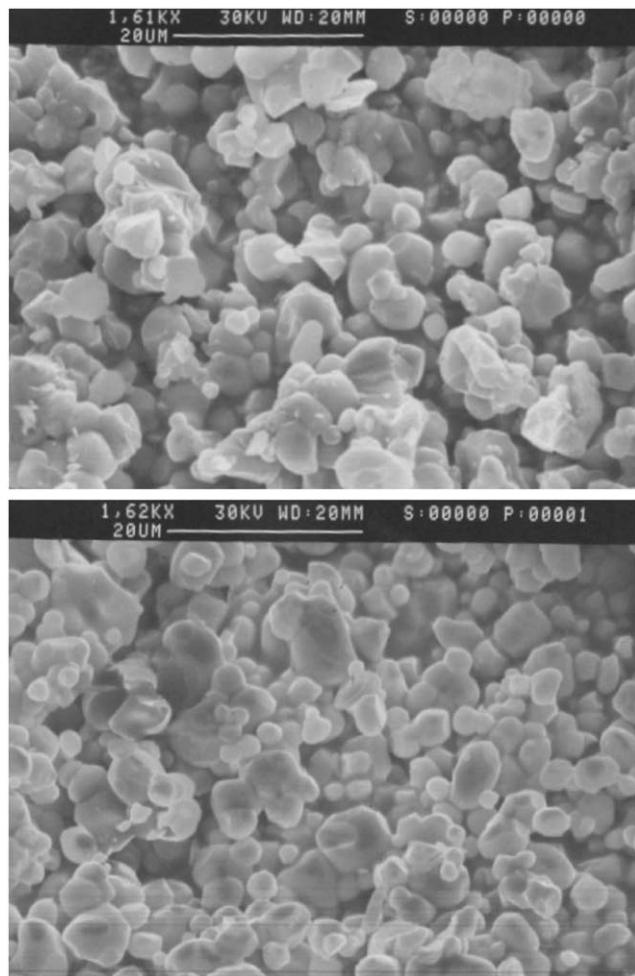


Fig. 1. SEM images of the $\text{Y}_{0.99}\text{Er}_{0.01}\text{VO}_4$ (upper panel) and $\text{Lu}_{0.99}\text{Er}_{0.01}\text{VO}_4$ (lower panel) compounds.

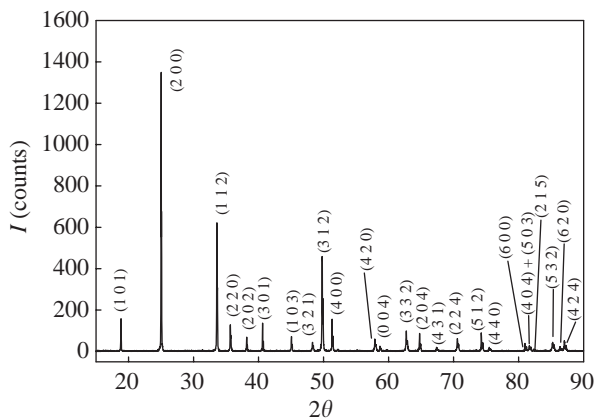


Fig. 2. Indexed powder diffraction pattern of $\text{Y}_{0.99}\text{Er}_{0.01}\text{VO}_4$. The pattern was indexed according to the JCPDS 82-1968 table.

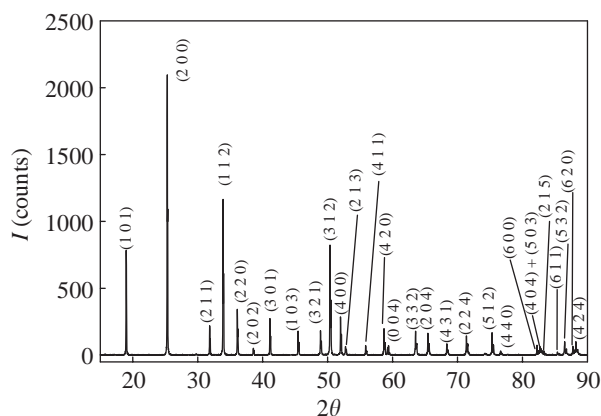


Fig. 3. Indexed powder diffraction pattern of $\text{Lu}_{0.99}\text{Er}_{0.01}\text{VO}_4$. The pattern was indexed as that of Fig. 2.

catalysis [9] and electrochemistry [10]. Both mono-dimensional (MAS and SATellite TRAnsition Spectroscopy, SATRAS) and two-dimensional (Multiple Quantum, MQMAS) experiments have been recently applied to the study of meta-, pyro- and ortho-vanadates [9,11–14]. In particular, it has been shown that the NMR spectra of orthovanadates are dominated by electric quadrupolar interaction (the quadrupolar coupling constant, C_Q , spans between 1 and 6 MHz), whereas the chemical shift anisotropy (CSA) is less than 100 ppm, due to the almost spherically symmetric shielding tensor of the tetrahedral oxygen environment (Q^0 unit) [9,14].

Figs. 4 and 5 show the ^{51}V MAS-NMR central lines of $\text{Y}_{0.99}\text{Er}_{0.01}\text{VO}_4$ and $\text{Lu}_{0.99}\text{Er}_{0.01}\text{VO}_4$, respectively. The δ -scales of the figures are referenced to the isotropic shifts, relative to VOCl_3 , given in Ref. [15]. The spectra of Figs. 4 and 5 are well fitted by a two-sites model: one accounting for vanadium in the normal Q^0 site, and another one due to vanadium tetrahedra perturbed by erbium. Table 1 reports the quadrupolar parameters

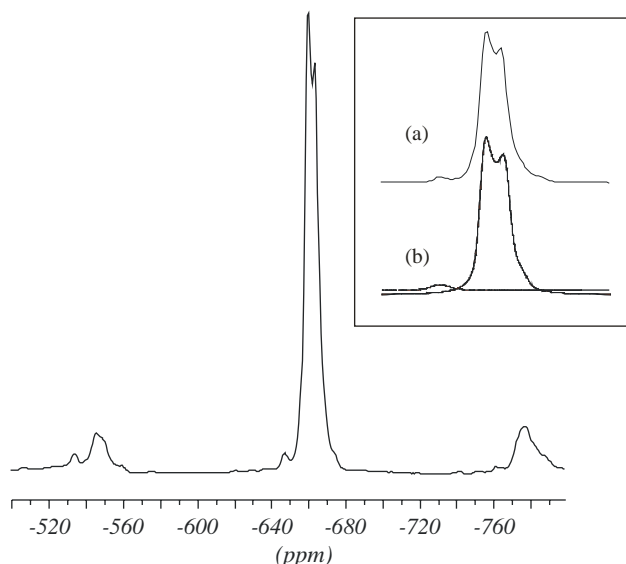


Fig. 4. ^{51}V MAS-NMR spectrum (central line) of $\text{Y}_{0.99}\text{Er}_{0.01}\text{VO}_4$. The inset shows an expansion of the line (a), together with its simulation (b, see text).

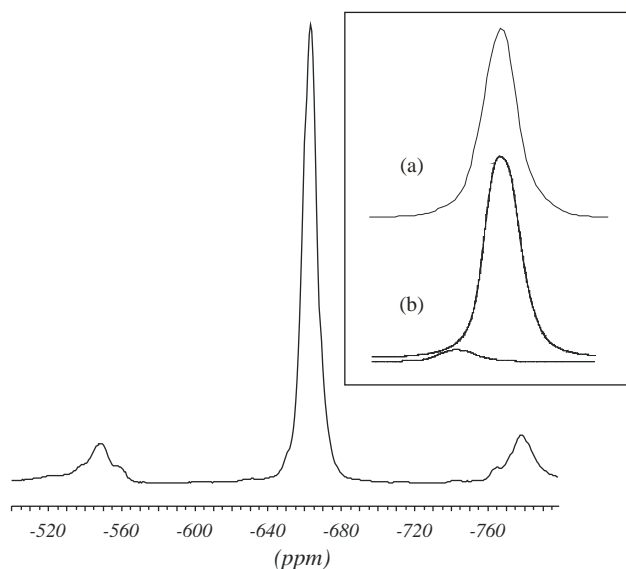


Fig. 5. ^{51}V MAS-NMR spectrum (central line) of $\text{Lu}_{0.99}\text{Er}_{0.01}\text{VO}_4$. The inset shows an expansion of the line (a), together with its simulation (b, see text).

obtained by the best-fit procedure. The parameters of the normal vanadium site (#1) are in good agreement with those reported in the literature [15], except for the asymmetry parameter of $\text{Lu}_{0.99}\text{Er}_{0.01}\text{VO}_4$, for which we obtained $\eta_Q = 0.4 \pm 0.2$ to be compared with the figure ~ 0 reported in the literature. The perturbed sites (#2) account for 2.3% and 3.4% of the total vanadium. From the crystal structure, we see that each vanadium Q^0 site shares edges with two rare earths polyhedra ($V-RE$ distance = 3.1 Å), and vertices with four RE polyhedra ($V-RE$ distance = 3.9 Å). If we suppose that all the RE are perturbing the V sites, irrespective from

Table 1
Parameters of ^{51}V MAS-NMR spectra

Compound		C_Q (MHz)	η_Q	Relative intensity (%)
$\text{Y}_{0.99}\text{Er}_{0.01}\text{VO}_4$	Site #1	4.76 ± 0.1	0.03 ± 0.05	97.7 ± 0.1
	Site #2	2.00 ± 0.2	1.00 ± 0.1	2.3 ± 0.1
$\text{Lu}_{0.99}\text{Er}_{0.01}\text{VO}_4$	Site #1	4.20 ± 0.1	0.4 ± 0.2	96.6 ± 0.1
	Site #2	4.8 ± 0.2	0.5 ± 0.1	3.4 ± 0.1

C_Q = quadrupolar coupling constant, η_Q = quadrupolar asymmetry parameter. The best fits have been performed on the central lines, and on three sidebands on each side of the main peak.

the distance, the expected probability for each V to be perturbed is $\sim 6\%$. In contrast, if we suppose that only the RE at 3.1 \AA have a noticeable effect on the quadrupolar parameters of the normal Q^0 site, the perturbation probability is reduced to $\sim 2\%$, in good agreement with the best fits of our NMR spectra. However, we stress that a correct estimation of the relative areas should be performed over all the spinning sidebands manifold [16], and not only over the central line plus the most intense sidebands, as we have made here for practical reasons. Our findings seem to point toward a homogeneous substitution of Erbium for Y and Lu in these compounds. In fact, other possibilities are: (i) non-homogeneous substitution (clustering) and (ii) interstitial occupancy with generation of cationic defects. The first possibility can be ruled out, since it would likely lead to a negligible number of perturbed vanadium Q^0 sites. The second one is also unlikely because of the very similar ionic radii of Er^{3+} (0.88 \AA), Y^{3+} (0.89 \AA) and Lu^{3+} (0.85 \AA). Moreover, the presence of cationic vacancies should lead to a distortion of the perturbed VO_4 tetrahedra, accompanied by a change of the quadrupolar parameters and, even, by an increase of the CSA [9]. This does not seem the case for $\text{Lu}_{0.99}\text{Er}_{0.01}\text{VO}_4$, since the quadrupolar parameters change less than 15%, and the spinning sidebands manifold does not show evidence of a larger CSA for site #2. In the case of $\text{Y}_{0.99}\text{Er}_{0.01}\text{VO}_4$, the situation is somehow different, since site #2 is characterized by a substantial reduction of C_Q and by an increase of η_Q . Whereas the reduction of the coupling constant goes contrariwise to an increased distortion of the VO_4 tetrahedra, at present we have not a clear-cut explanation for the increase of η_Q . Again, no variations of the CSA pattern are observed.

Fig. 6 shows the ^{89}Y MAS-NMR spectrum of $\text{Y}_{0.99}\text{Er}_{0.01}\text{VO}_4$. A single peak is observed with an isotropic chemical shift of -66 ppm , and a full-width at half-height (FWHM) of about 120 Hz. Although ^{89}Y is a favorable spin- $\frac{1}{2}$ nucleus, to date NMR studies are very scarce because of its low gyromagnetic ratio ($\sim 2.09 \text{ MHz/T}$), long relaxation times, and severe probe ringing which is generally observed at low frequencies ($< 30 \text{ MHz}$). While a number of wide-line and low-

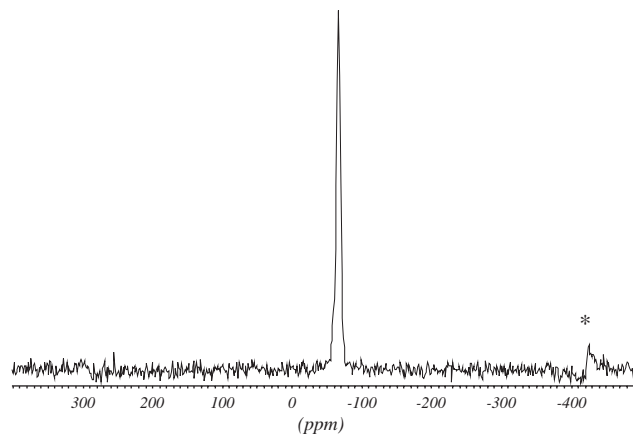


Fig. 6. ^{89}Y MAS-NMR spectrum of $\text{Y}_{0.99}\text{Er}_{0.01}\text{VO}_4$. The asterisk marks a spinning sideband.

temperature studies have been reported on Y-containing ceramic superconductors (see, e.g., [17]) and magnetic materials (see, e.g., [18]), only a few papers appeared about MAS studies of diamagnetic oxides. Grey et al. [19] studied the effects of the incorporation of large amounts of paramagnetic lanthanides in diamagnetic pyrochlores $\text{Y}_2\text{M}_2\text{O}_7$ ($M = \text{Sn, Ti}$), showing that the addition of the Ln ions caused the appearance of additional resonances. Becerro et al. [20] recently correlated the chemical shifts and the coordination numbers of yttrium in silicates. Our present results confirm the presence in the orthovanadate structure of a unique Y site, whose chemical shift is compatible with the YO_8 coordination expected for the $4b$ position of $I4_1/amd$ space group. No evidence is found of an yttrium site perturbed by neighboring ErO_8 polyhedra, although each REO_8 bisdisphenoid “sees” four similar sites as the first neighbors. This finding may be unexpected, above all if compared with the findings of Ref. [19] and with our present ^{51}V results, but can be rationalized by considering that: (i) the substitution in our samples is of 1%, against 30% of Grey et al. [19], and (ii) the ^{89}Y spin- $\frac{1}{2}$ spectrum is less sensitive than the ^{51}V quadrupolar one to the local distortions caused by erbium-for-yttrium substitution in the second coordination sphere.

4. Conclusions

The synthesis of the $Y_{0.99}Er_{0.01}VO_4$ and $Lu_{0.99}Er_{0.01}VO_4$ materials was successfully accomplished by solid-state reaction starting from the parent oxides. The reaction was carried out at 800 °C in air. Firing the starting mixture for 12 h was found sufficient to complete the reaction, and to obtain well-crystallized and homogeneous materials, as demonstrated by XRPD measurements and SEM-EMPA inspection of the products.

The MAS-NMR characterization points toward the substitutional nature of erbium on the *RE* site. In particular, as expected, the quadrupolar probe (^{51}V) is more sensitive than the spin- $\frac{1}{2}$ one (^{89}Y) in revealing the small distortions caused by erbium–yttrium substitution in the REO_8 bisdisphenoids. The isotropic chemical shift of ^{89}Y in an orthovanadate is reported for the first time in the literature.

Acknowledgments

This work has been partially supported by the Italian Ministry of University and Research by means of the “PRIN, Materiali nanostrutturati luminescenti attivati con ioni lantanidi” project. We are grateful to K. Eichele for the WSOLIDS program.

R.A. acknowledges a grant from Italian Ministry of University and Research (PRIN 2003).

References

- [1] K.J. Range, H. Meister, U. Klement, Z. Naturforsch. B 45 (1990) 598.
- [2] J.A. Baglio, O.J. Sovers, J. Solid State Chem. 3 (1971) 458.
- [3] H. Fuess, A. Kallel, J. Solid State Chem. 5 (1972) 11.
- [4] A. Patscheke, H. Fuess, G. Will, Chem. Phys. Lett. 2 (1968) 47.
- [5] G. Will, W. Schafer, J. Phys. C Solid State Phys. 4 (1971) 811.
- [6] B.C. Chakoumakos, M.M. Abraham, L.A. Boatner, J. Solid State Chem. 109 (1994) 197.
- [7] G. Spinolo, F. Maglia, Powder Diffraction 14 (1999) 208.
- [8] WSOLIDS package was provided by K. Eichele. See: <http://casgm3.anorg.chemie.uni-tuebingen.de/klaus/soft/index.html>.
- [9] O.B. Lapina, A.A. Shubin, D.F. Khabibulin, V.V. Terskikh, P.R. Bodart, J.-P. Amoureux, Catal. Today 78 (2003) 91.
- [10] P.E. Stallworth, X. Guo, E. Tatham, S.G. Greenbaum, M. Arrabito, S. Bodoarado, N. Penazzi, Solid State Ionics 170 (2004) 181.
- [11] J. Skibsted, C.J.H. Jakobsen, H. Jakobsen, Inorg. Chem. 37 (1998) 3083.
- [12] U.G. Nielsen, H.J. Jakobsen, J. Skibsted, Inorg. Chem. 39 (2000) 2135.
- [13] U.G. Nielsen, H.J. Jakobsen, J. Skibsted, J. Phys. Chem. B 105 (2001) 420.
- [14] U.G. Nielsen, H.J. Jakobsen, J. Skibsted, Solid State Nucl. Magn. Reson. 23 (2003) 107.
- [15] O.B. Lapina, V.M. Mastikhin, A.A. Shubin, V.N. Krasilnikov, K.I. Zamaraev, Progress in NMR Spectroscopy, vol. 24, Pergamon Press, London, 1992, p. 457.
- [16] C. Jäger, Satellite Transition Spectroscopy of Quadrupolar Nuclei, in: P. Diehl, et al. (Eds.), Solid State NMR II: Inorganic Matter, Springer, Berlin, 1994, p. 133.
- [17] M. Mali, et al., J. Supercond. 15 (2002) 511; J. Bobroff, et al., Phys. Rev. Lett. 89 (2002) 157002; P.M. Singer, T. Imai, Phys. Rev. Lett. 88 (2002) 187601; A.Y. Zavidonov, D. Brinkmann, Phys. Rev. B 63 (2001) 132506.
- [18] J.H. Cho, et al., J. Magn. Magn. Mater. 272–276 (2004) 970; G.I. Drandova, et al., J. Low. Temp. Phys. 131 (2003) 305; A. Keren, J.S. Gardner, Phys. Rev. Lett. 87 (2001) 177201.
- [19] C.P. Grey, M.E. Smith, A.K. Cheetam, C.M. Dobson, R. Dupree, J. Am. Chem. Soc. 112 (1990) 4670.
- [20] A.I. Becerro, A. Escudero, P. Florian, D. Massiot, M.D. Alba, J. Solid State Chem. 177 (2004) 2783.